

Secondary photorefractive centers in $\text{Sn}_2\text{P}_2\text{S}_6:\text{Sb}$ crystals

Dean R. Evans,¹ Alexandr Shuymelyuk,^{2,*} Gary Cook,^{1,3} and Serguey Odoulov²

¹Air Force Research Laboratory, Materials and Manufacturing Directorate,
Wright-Patterson Air Force Base, Ohio 45433, USA

²Institute of Physics, National Academy of Sciences, 03 650 Kyiv, Ukraine

³Azimuth Corporation, 4134 Linden Avenue, Suite 300, Dayton, Ohio, USA

*Corresponding author: shumeluk@iop.kiev.ua

Received November 9, 2010; accepted December 13, 2010;
posted January 10, 2011 (Doc. ID 137923); published February 2, 2011

Secondary photorefractive centers in Sb-doped $\text{Sn}_2\text{P}_2\text{S}_6$ have a lifetime comparable to the formation time of the space-charge grating. This considerably affects the dynamics of two-beam coupling and results in a new type of transient gain enhancement for preilluminated samples. © 2011 Optical Society of America

OCIS codes: 190.5330, 160.2260.

Since the beginning of the 1990s, the presence of shallow secondary photorefractive centers in BaTiO_3 and similar materials has been proved in a convincing manner [1–3]. It was shown that population of initially empty shallow traps by light results in nonlinear absorption, nonlinear photoconductivity, unusual intensity dependence of the grating decay time (I^x , x less than 1), and intensity dependence of the gain factor. The proposed models [1–3] explained the experimental results quite well within the assumption that the lifetime of shallow secondary centers, τ_{sec} , is much smaller than the buildup and photo-induced decay of the space-charge grating, $\tau_{\text{sec}} \ll \tau_{\text{sc}}$.

It was later discovered that photorefractive crystals may possess more deep secondary centers, with the lifetime of the trapped carrier largely exceeding the lifetime of the space-charge grating, $\tau_{\text{sec}} \ll \tau_{\text{sc}}$. A nominally undoped $\text{Sn}_2\text{P}_2\text{S}_6$ sample, for example, can be sensitized to near-IR recording via pre-exposure to white light [4]. The lifetime of the secondary centers that are responsible for the increased sensitivity to near-IR light in these crystals is $\tau_{\text{sec}} \approx 10^5$ s (compared with $\tau_{\text{sc}} \approx 10$ s, typical for near-IR recording).

Being deliberately populated with the auxiliary light, these relatively deep secondary centers affect the Debye screening length and improve the sensitivity, but they do not result in intensity-dependent two-beam coupling gain and the other abovementioned effects, which are typical manifestations of shallow traps.

This Letter reports on an unusual manifestation of the photorefractive effect in Sb-doped $\text{Sn}_2\text{P}_2\text{S}_6$ (SPS:Sb) crystals [5] (strong transient extinction of the transmitted light beam in a sample pre-exposed to intense light of the same wavelength, strong dependence of the two-beam-coupling dynamics on the sample prehistory, and sensitivity of transient extinction even to the ambient light of the laboratory) that we attribute to the presence of *secondary centers with a lifetime that is comparable to the formation time of the space-charge grating*, $\tau_{\text{sec}} \approx \tau_{\text{sc}}$. Although not yet identified, the secondary centers in SPS:Sb are optically characterized, their lifetime is estimated from the study of transient beam fanning, and their activation energy is found from measurements at different temperatures.

The SPS crystals are promising photorefractive crystals with a short response time and quite a strong Pockels

effect [6], grown at Uzhgorod National University, Ukraine. The samples of SPS:Sb are cut along the crystallographic axes, and their faces are optically finished. Qualitatively, all tested samples behave in a similar way. In this Letter, the data are presented for two samples, thick and thin, measuring respectively 7.5 and 4 mm along the y axis. A He–Ne laser (TEM_{00} , $\lambda = 0.63 \mu\text{m}$) is used as a light source.

When we studied two-beam coupling, an unexpected behavior was revealed. In addition to regular beam coupling with a direction that depends on the polar axis orientation, we saw an increase of the signal intensity with the pump beam switched on and strong transient extinction after the pump beam was switched off. These bleaching and darkening effects were insensitive to the polar axis inversion. By choosing the polarization of the pump beam to be orthogonal, it was possible to eliminate regular beam coupling while still preserving bleaching and darkening effects. Moreover, with fixed parameters of the weak signal beam (orientation, polarization, intensity) the new effects were practically insensitive to the orientation of the strong pump beam, which could be copropagating or counterpropagating to the signal beam or even entering the sample through the side faces. The probe beam along the y axis was polarized along the x axis.

Figure 1 shows the intensity of the probe beam transmitted through the thick sample after switching off the strong pump beam. Different curves are measured with an increasing time interval, Δt , between switching off the pump beam and switching on the weak signal beam. During this time, Δt , the sample is kept in the dark. It is evident that the probe extinction is not instantaneous; it develops gradually in time and disappears slowly. The strongest extinction corresponds to the smallest delay; it becomes less pronounced for increasing Δt . At the same time, the decay rate of transient extinction practically does not depend on Δt .

The strength of extinction depends on the intensity of the probe beam itself (Fig. 2). The smaller the intensity, the less pronounced the extinction, which roughly disappears for input probe power below 0.1 mW/cm^2 .

It was found that the probe extinction is caused by a strong transient fanning from this beam. The fanning develops directly after pre-exposure of the sample to the

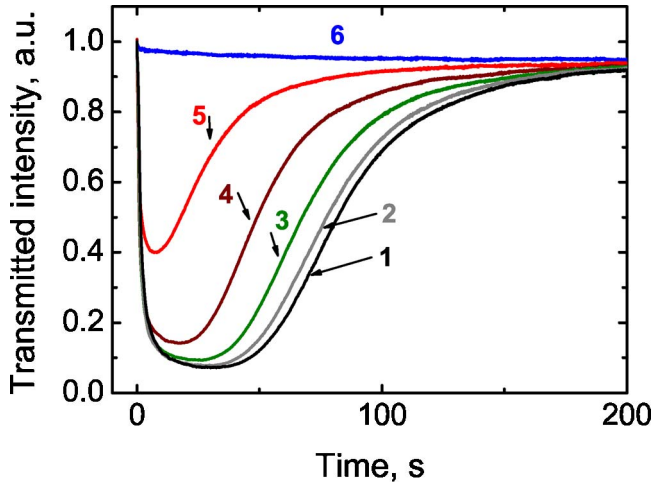


Fig. 1. (Color online) Temporal variation of the probe beam intensity after pre-exposure of the thick sample to the strong pump beam. Time traces from 1 to 6 correspond to time delays of 1, 10, 25, 50, 100, and 200 s between switching off the pump beam and switching on the probe beam, respectively. $I_{\text{probe}}^0 = 3 \text{ mW/cm}^2$ and $I_{\text{pump}} = 2 \text{ W/cm}^2$.

strong pump beam. It becomes smaller if the probe beam is switched with a delay and saturates for $\Delta t \geq 200 \text{ s}$. The weak extinction of the probe beam, shown as curve 6 in Fig. 1, is due to a steady state fanning.

Thus we conclude that the pre-exposure of SPS:Sb to a strong pump beam has two consequences: (i) it washes out all noisy scattering gratings induced by the probe beam (the reason why the initial value of the transmitted probe intensity in Fig. 1 is larger than its saturated value at $t \geq 200 \text{ s}$); and (ii) it improves the sample sensitivity, which considerably increases the gain factor. From the fact that the probe extinction and the induced fanning are both transient, we conclude that their disappearance in the steady state is caused by the limited lifetime of the secondary centers, responsible for the gain enhancement.

The transient beam fanning occurs within a certain intensity range of the probe beam. If the probe intensity is so small that photoconductivity becomes comparable to the dark conductivity, the enhanced gain is reduced and scattering does not develop (curves 6 and 7 in Fig. 2). We discovered that the probe intensity level at which the fanning (and sample darkening) becomes undetectable depends on the ambient light in the laboratory, which increases the effective dark conductivity. On the other hand, the probe beam with high intensity should saturate the population of secondary centers and both fanning and extinction should not vanish with time.

The lifetime of the secondary centers, τ_{sec} , is estimated from the data in Fig. 1. The transmitted probe intensity can be represented as follows:

$$I_s = I_s^0 - I_{\text{tf}} - I_{\text{cf}}, \quad (1)$$

where I_s^0 is the intensity at $t = 0$, I_{tf} is the intensity of transient fanning that develops in the pre-exposed sample and fades away when the gain factor returns to its basic value typical for the virgin sample, and I_{cf} is the intensity of conventional fanning that is related to the basic gain factor.

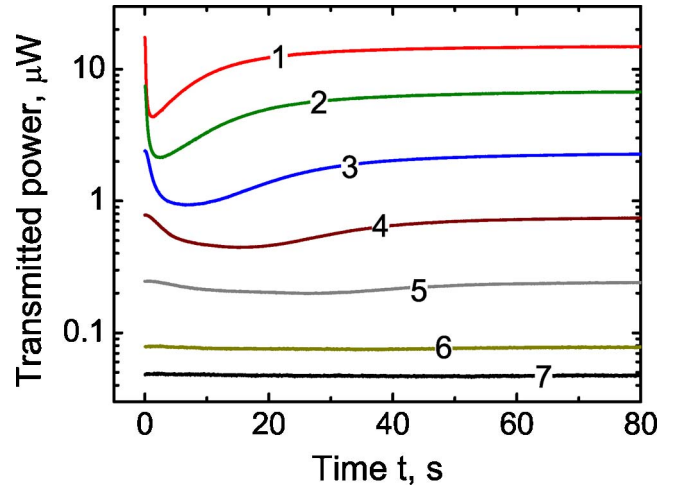


Fig. 2. (Color online) Temporal variation of the transmitted probe beam power after pre-exposure of the sample to the strong pump beam. Time traces from 1 to 7 correspond to the incident probe intensities 17, 7, 2.2, 0.75, 0.25, 0.08, and 0.04 mW/cm^2 , respectively. $\Delta t = 0.5 \text{ s}$, $I_{\text{pump}} = 2 \text{ W/cm}^2$, thin sample.

The changes of the gain factor in SPS occur because of strong screening, which is due to a trap density limitation [4,7,8]. In such a case and for reasonably weak coupling, the fanning intensity I_{tf} at the tails of the light-induced darkening should be proportional to the gain factor, Γ . The gain factor, in turn, should be proportional to the effective trap density; see, e.g., Eq. (2) in [8]:

$$I_{\text{tf}}(t) \propto N_{\text{eff}} \exp(-t/\tau_{\text{sec}}). \quad (2)$$

By fitting Eq. (2) to the tails of the vanishing darkening effect we get $\tau_{\text{sec}} = 14 \pm 1 \text{ s}$ for both SPS:Sb samples.

Although τ_{sec} is relatively long compared to the buildup time of the fast grating in SPS ($\approx 0.2 \text{ s}$ for our intensities), it is comparable to the characteristic time of the slow compensating grating [4], which is usually on the order of tens of seconds. Such a time hierarchy has never been observed, to our best knowledge, in other photorefractive crystals. This particularity of SPS:Sb may complicate the two-beam-coupling dynamics. One example is given in Fig. 3, where the temporal evolutions are shown for [Figs. 3(a) and 3(b)] the weak signal beam during the grating recording and [Figs. 3(c) and 3(d)] the decay of the diffracted beam when the signal beam is switched off. For Fig. 3(a) the signal beam is sent to the sample at $t = 0$, when the sample was already illuminated by the pump beam, while for Fig. 3(b), the pump and the signal beams are switched on simultaneously at $t = 0$. Figures 3(c) and 3(d) correspond to Figs. 3(a) and 3(b), respectively, showing the decay of the gratings, which were recorded under different initial conditions.

The dramatic difference in the dynamics of grating recording is obvious: the signal beam intensity reaches its saturation value within less than a second for the sample pre-exposed to the pump beam [Fig. 3(a)], while it takes more than 10 s if the two beams start to record a grating in a virgin sample [Fig. 3(b)]. The buildup of the beam coupling in Fig. 3(b) reflects the slow growth of the effective trap density. Its characteristic time is much larger than that of the fast grating recording.

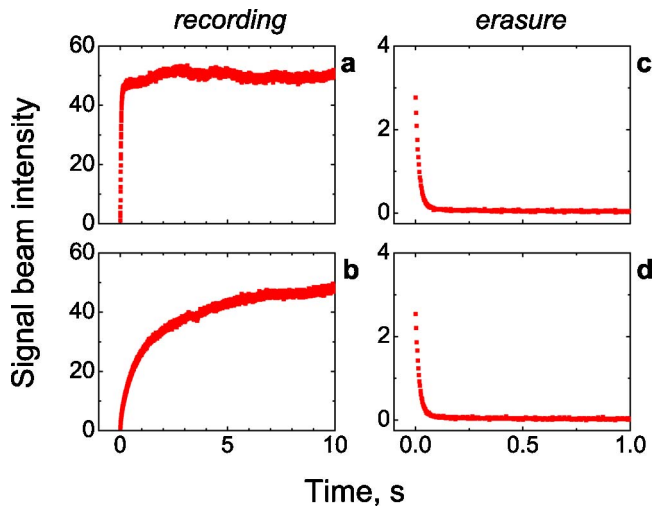


Fig. 3. (Color online) Temporal variation of the signal intensity during grating (a and b) recording and (c and d) erasure. For a, the signal beam is introduced at $t = 0$ to the sample pre-exposed with the strong pump beam, while for b, both beams are switched on at $t = 0$. c and d show the diffracted beam intensity when the signal beam is switched off at $t = 0$, after saturation is reached in a and b. $\Lambda = 0.8 \mu\text{m}$, $I_{\text{pump}} = 2 \text{ W/cm}^2$, thin sample.

Note that two decay curves, Figs. 3(c) and 3(d), are identical, which is expected because in both cases the initial conditions are the same. Here the sample is illuminated by the strong pump beam well before $t = 0$.

We selected the recording-erasure dynamics for the grating with grating spacing $\Lambda = 0.8 \mu\text{m}$ for Fig. 3, where the amplitude of compensation grating is virtually invisible. An apparent difference in the recording dynamics for the virgin and pre-exposed samples is observed also for a larger grating spacing, $\Lambda = 9.5 \mu\text{m}$, where the compensation grating is well pronounced.

The measurements of the lifetimes within the temperature range from -16 to $47 \text{ }^\circ\text{C}$ allowed for the determination of the activation energy, $\Delta E \approx 0.33 \text{ eV}$ (Fig. 4).

To summarize, our results confirm the conclusion that Sb doping leads to an enhancement of beam coupling in SPS for red light [5]. They reveal nontrivial dynamics of beam coupling and beam fanning, which we attribute to a particular lifetime of secondary charge traps.

Any SPS crystal possesses, most probably, a multitude of secondary centers with a wide range of lifetimes. The dominant traps among this variety manifest themselves in wave mixing more strongly than others. For SPS:Pb, only the short-living traps reveal themselves [9] in the intensity-dependence of the Debye screening length. For nominally undoped SPS, two types of traps were detected: the short-living that are responsible for the intensity dependence of the gain factor [7] and also long-living traps responsible for light-induced sensitizing [4]. SPS:Sb is the only presently known photorefractive

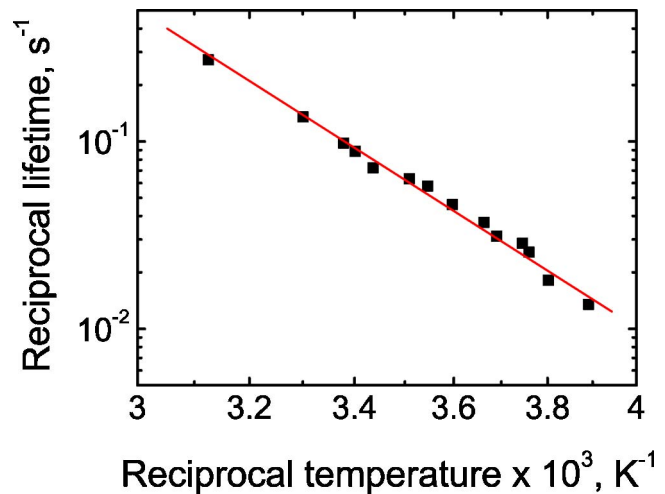


Fig. 4. (Color online) Arrhenius plot for determination of the activation energy of secondary centers. The decay rates, τ^{-1} , are extracted from the dependences similar to those shown in Fig. 1, but measured at different temperatures.

material for which the lifetime of photogenerated traps is comparable to the formation time of the space-charge grating. This particularity of SPS:Sb should be taken into account in its possible applications as, e.g., for reconfigurable optical interconnects [10].

The authors thank A. Grabar and I. Stoyka for SPS samples. A part of this work has been done during the stay of D. Evans at the Institute of Physics, Kiev, Ukraine. Financial support from the European Office of Research and Development via the Science and Technology Center, Ukraine (P335) is gratefully acknowledged.

References

1. G. A. Brost, R. A. Motes, and J. R. Rotge, *J. Opt. Soc. Am. B* **5**, 1879 (1988).
2. L. Holtmann, *Phys. Status Solidi A* **113**, K89 (1989).
3. P. Tayebati and D. Mahgerefteh, *J. Opt. Soc. Am. B* **8**, 1053 (1991).
4. S. Odoulov, A. Shumelyuk, U. Hellwig, R. Rupp, and A. Grabar, *J. Opt. Soc. Am. B* **13**, 2352 (1996).
5. T. Bach, M. Jazbinsek, G. Montemezzani, P. Günter, A. Grabar, and Yu. Vysochanskii, *J. Opt. Soc. Am. B* **24**, 1535 (2007).
6. A. Grabar, M. Jazbinsek, A. Shumelyuk, Yu. M. Vysochanskii, G. Montemezzani, and P. Günter, in *Photorefractive Materials and Their Applications 2*, P. Günter and J.-P. Huignard, eds. (Springer, 2007), pp. 327–362.
7. A. Shumelyuk, M. Wesner, M. Imlau, and S. Odoulov, *Appl. Phys. B* **95**, 497 (2009).
8. A. Shumelyuk, S. Odoulov, G. Cook, and D. R. Evans, *Opt. Lett.* **34**, 2126 (2009).
9. A. Shumelyuk, D. Barilov, M. Imlau, A. Grabar, I. Stoyka, and Yu. Vysochanskii, *Opt. Mater.* **30**, 1555 (2008).
10. Y. Wakayama, A. Okamoto, K. Shimayabu, Y. Kojima, and A. Grabar, *Proc. SPIE* **7212**, Q1 (2009).